

Chimia 51 (1997) 140–144  
 © Neue Schweizerische Chemische Gesellschaft  
 ISSN 0009–4293

# Dynamics of Biomolecules Studied by NMR Relaxation Spectroscopy

Rafael Brüschweiler\*

(Werner Prize 1996 of the NSCS)

**Abstract.** New developments in nuclear magnetic resonance (NMR) relaxation spectroscopy and the availability of isotopically labeled biomolecules led to significant progress in the understanding of polypeptide dynamics in solution. This article summarizes some of the author's work on homonuclear and heteronuclear NMR relaxation of peptides and proteins and their structural dynamical interpretation based on a variety of different methods.

## Introduction

The function of biomolecules, such as peptides, proteins, and nucleic acids, is invariably coupled to structural flexibility and molecular motion. Examples include binding of ligands, such as ions, molecular recognition, important, *e.g.* for protein-DNA interactions that regulate transcription, or enzymatic activity, where a substrate typically binds to the receptor following the principle of 'induced fit'. Besides a kinematic view of molecular motion aiming at a description with high resolution in space and time, there is also the thermodynamic perspective (*Scheme*). Roughly, enthalpy is a function of the average three-dimensional structure while entropy is a function of molecular dynamics, which together determine the free energy that drives the actions of the system.

Molecular motion is highly sensitive to the environment, suggesting that biomolecular dynamics studies should be carried out in the native environment, which is often in solution. A unique method that can provide very detailed dynamical information on the solution state is nuclear magnetic resonance (NMR) relaxation spectroscopy [1–3]. From spin- $1/2$  nuclei, such as  $^1\text{H}$ ,  $^{13}\text{C}$ , and  $^{15}\text{N}$ , the dominant intramolecular spin interaction is the pairwise magnetic dipolar coupling, depicted in *Fig. 1*, depending on the internuclear distance  $r_{IS}$  as well as on the angle  $\theta_{IS}$

between the internuclear vector and the external static magnetic field  $B_0$

$$H_{IS}^D \propto \frac{3 \cos^2 \theta_{IS} - 1}{r_{IS}^3} \quad (1)$$

The dipolar interaction causes transfer of polarization between spins. This process is manifested in multidimensional proton-proton cross-relaxation NMR experiments (NOESY) [4], which form the basis of three-dimensional (3D) protein structure determination by NMR [5][6]. Reorientational molecular motion leads to stochastic time modulation of the dipolar interaction, which induces energy exchange between the spin system and the lattice [7]. This mechanism causes a non-equilibrium spin state, that was previously prepared by the application of radio-frequency (rf) pulses, to relax towards thermal equilibrium. Due to its sensitive dependence on the motional timescales and amplitudes, this process provides a 'fin-

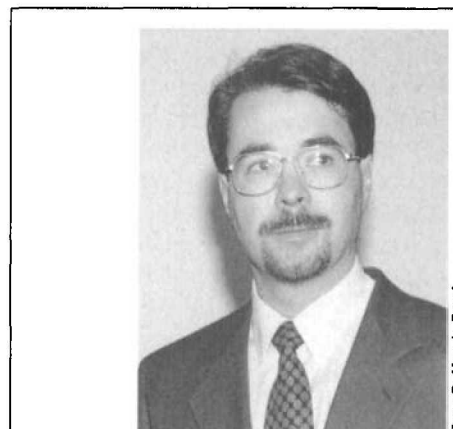


Foto: R. Hauck, Basel

Rafael Peter Brüschweiler, born 1962 in Zürich, studied physics at ETH, where he graduated in 1986 with a diploma thesis in solid-state physics. For his Ph.D. thesis, he joined the group of Prof. Richard R. Ernst at the Laboratorium für Physikalische Chemie at ETH working on nuclear magnetic resonance (NMR) relaxation methodology and its application to structural dynamics of biomolecules. After receiving his Ph.D. in 1991, which was awarded with the ETH Silver Medal, he moved with a fellowship from the Swiss National Science Foundation to The Scripps Research Institute in La Jolla, California, where he worked with Dr. Peter E. Wright and Dr. David A. Case on protein dynamics by using NMR and computer simulations. In 1994, he returned as Oberassistent to the Laboratorium für Physikalische Chemie at ETH. In 1996, he received the Werner Prize of the New Swiss Chemical Society.

gerprint' of the dynamics probed at the molecule's many different nuclear sites carrying a spin.

## Homonuclear Cross Relaxation

In NOESY proton-proton cross-relaxation experiments, intramolecular motion is manifested by angular and radial modulation of the dipolar interactions [8]. Angular modulation is caused by the overall rotational diffusion motion ('rotational tumbling') as well as by internal motion,

*Scheme*

## How do biomolecules work?

*kinematic picture*

Structure + Dynamics  $\longrightarrow$  Function

*thermodynamic picture*

Enthalpy - T × Entropy = Free Energy

\*Correspondence: Dr. R. Brüschweiler  
 Laboratorium für Physikalische Chemie  
 ETH-Zentrum  
 CH-8092 Zürich

while radial modulation is purely due to internal dynamics. For internal motional timescales  $\tau_{int}$  much slower than the inverse Larmor frequency, lying *e.g.* in the  $\mu\text{s}$ – $\text{ms}$  range, the cross-relaxation rate constant between spins  $i$  and  $j$  with time-dependent distance  $r_{ij}(t)$  is proportional to the  $\langle r_{ij}^{-6} \rangle$  average independent of the internal timescale. Since for these timescales only one set of NMR lines is visible, identification of multiple conformations often relies on indirect methods: A clear indication of conformational averaging is the inexistence of a physically realistic single conformer whose 3D structure is compatible with all NOESY proton-proton distance constraints. Since most computer algorithms in the field [6][9] that are being used for the determination of 3D protein structures intrinsically search for single structures, which simultaneously fulfill all distance constraints, the characterization of multiconformational equilibria requires a different strategy. One strategy was implemented in the protocol MEDUSA [10].

MEDUSA consists of three main steps: In a first step, a large number of physically viable conformations is generated, each of them partially fulfilling a subset of NOESY distance constraints. In a second step, the generated conformations are clustered for reasons of data reduction. In a third step, population-weighted conformational ensembles are identified which quantitatively best fulfill the experimental data.

The protocol was applied to the hydrophobic cyclic decapeptide antamanide ( $-^1\text{Val}-^2\text{Pro}-^3\text{Pro}-^4\text{Ala}-^5\text{Phe}-^6\text{Phe}-^7\text{Pro}-^8\text{Pro}-^9\text{Phe}-^{10}\text{Phe}-$ ) dissolved in chloroform. Antamanide is an antidote against the poisonous mushroom *Amanita phalloides*, which was known previously to undergo conformational exchange [11]. The two best-fitting pair conformations that were obtained by MEDUSA can be characterized according to *syn*-correlated and *anti*-correlated flips in the  $\varphi_5$ ,  $\varphi_{10}$ -backbone dihedral angles, respectively [10]: Fig. 2 shows stereographic views of the *syn*-correlated pair (top) and the *anti*-correlated pair (bottom) exhibiting different hydrogen-bonding networks indicated by dashed lines. In addition,  $T_{1\rho}$ -dispersion measurements indicate interconversion times at room temperature in the  $\mu\text{s}$ -range [10].

### Heteronuclear Relaxation

Relaxation of a  $^{13}\text{C}$  or  $^{15}\text{N}$  spin is usually dominated by the dipolar interaction to the directly attached proton. Relax-

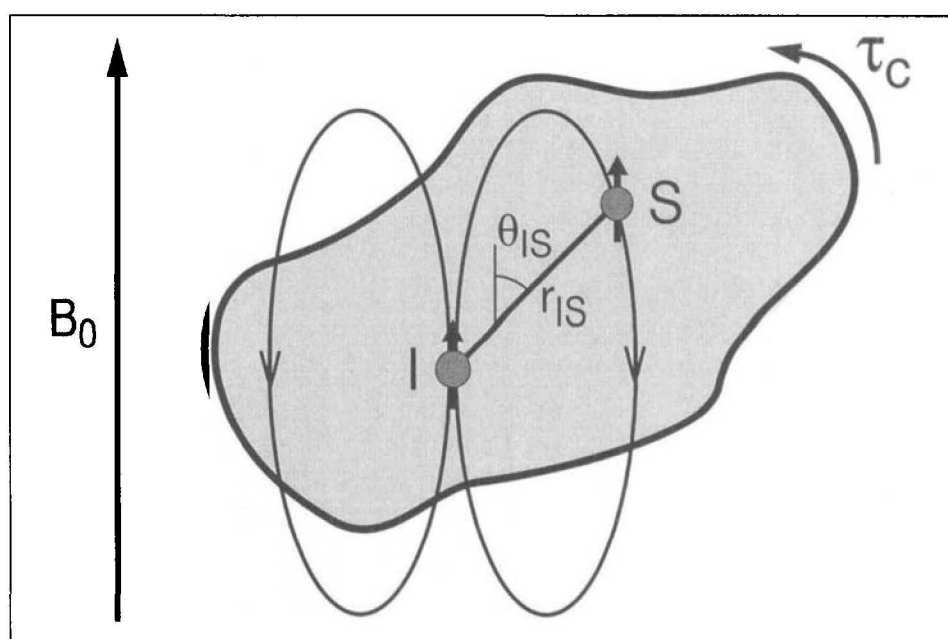


Fig. 1. Magnetic dipole-dipole interaction between nuclear spins I and S that are part of a tumbling molecule

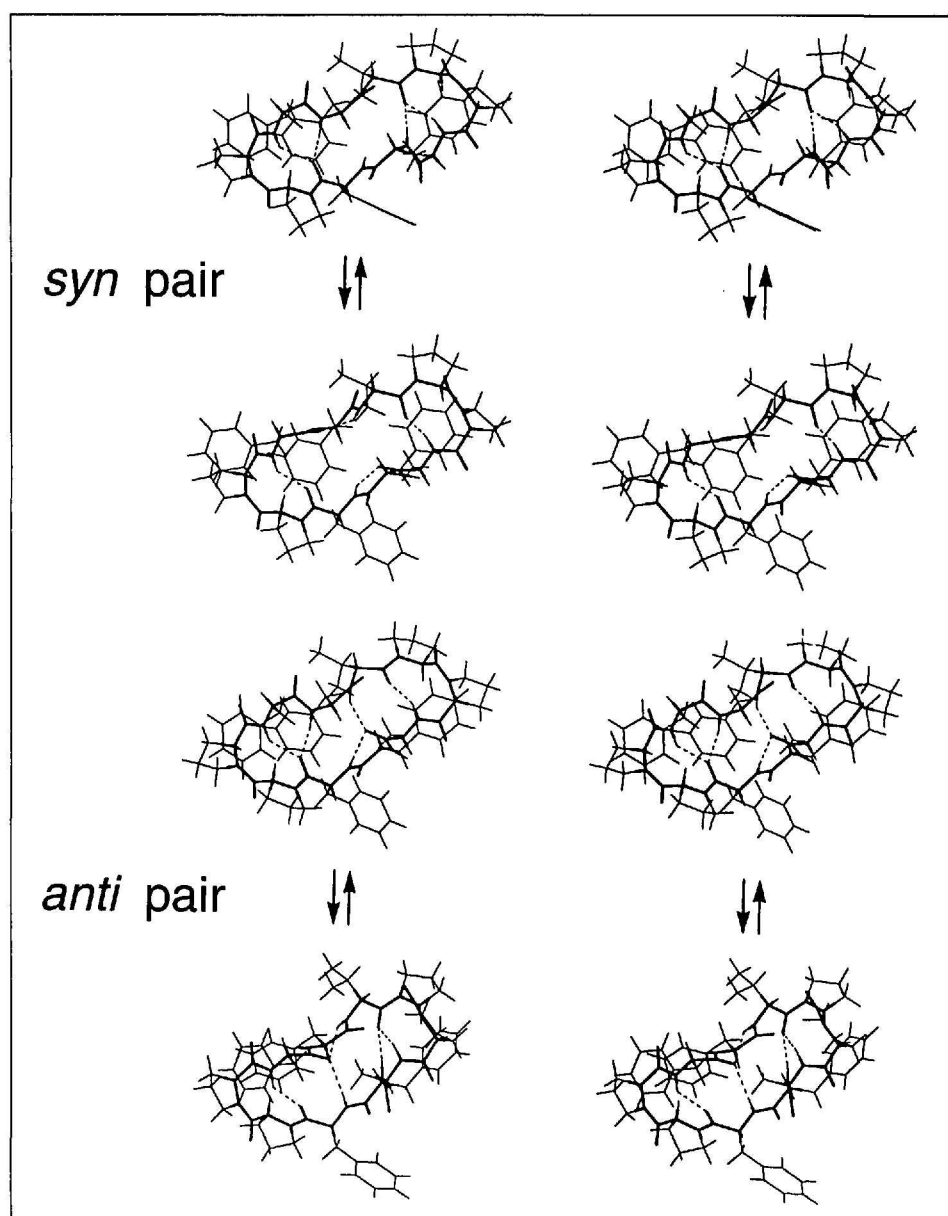


Fig. 2. Stereographic pictures of the best-fitting conformational pairs of antamanide. Top: *syn*-pair; bottom: *anti*-pair (reprinted with permission from [10b]).

ation parameters, such as the longitudinal relaxation time  $T_1$  and the transverse relaxation time  $T_2$ , and the heteronuclear NOE can be measured for each heteronucleus using NMR pulse sequences [12] schematically shown in Fig. 3. For sensitivity reasons, magnetization is transferred from the protons to the heteronuclei, where

during the  $t_1$ -evolution period the heteronuclei are frequency-labelled. Then follows a variable delay  $\tau_m$ , during which magnetization is allowed to relax, before the remaining magnetization is transferred back to the protons for detection. Two-dimensional Fourier transformation along the  $t_1, t_2$  dimensions [4] yields the neces-

sary resolution to measure cross-peak amplitudes for increasing  $\tau_m$  that allow extraction of  $T_1$  and  $T_2$  relaxation parameters as decay times of exponential curves lying typically in the 0.01–1-s range.

### Relaxation Data Interpretation

Since heteronuclear radial modulation is quite weak and uniform, differential effects in the heteronuclear relaxation data can be unambiguously attributed to angular motion. Over the years, different classes of motional models have been developed. While for overall tumbling either isotropic or anisotropic rotational diffusion is feasible (see next section), for internal motion, one can distinguish between 1) concrete analytical models, 2) abstract analytical models, and 3) molecular force-field-based models (computer simulations).

Since experimental data alone often do not allow one to discriminate between different concrete analytical models, e.g. jump model vs. diffusion model, the 'model-free' description [13] has become popular as an alternative description of protein relaxation data. In this approach, the relaxation parameters are translated to abstract parameters that separately reflect spatial and timescale motional effects: an order parameter  $S^2$ , which is a measure for the spatial restriction of the internuclear vector, and an effective internal correlation time  $\tau_{int}$  [13]. In the absence of intramolecular motion  $S^2 \approx 1$ , whereas  $S^2 \ll 1$  reflects a large amount of intramolecular motion. Experimentally observed  $\tau_{int}$  values usually fall into the subnanosecond range.

It can be shown [14] that

$$S^2 = \frac{4\pi}{5} \sum_{m=-2}^2 \sigma_{Y_{2m}}^2 \quad (2)$$

where the  $\sigma_{Y_{2m}}^2 = \langle Y_{2m} Y_{2m}^* \rangle - \langle Y_{2m} \rangle \langle Y_{2m}^* \rangle$  are the 2nd moments of the spherical harmonics  $Y_{2m}$  evaluated over the spatial distribution of the corresponding internuclear vector. Eqn. 2 also illuminates the relationship between NMR  $S^2$  values and X-ray crystallographic temperature factors  $B \propto \sum_{m=-1}^1 \sigma_{rY_{1m}}^2$ . Like  $S^2$ ,  $B$  reflects 2nd moment information, but unlike  $S^2$ ,  $B$  is also sensitive to purely translational motion due to the  $r$  dependence in the  $rY_{1m}$  terms.

It is clear that from 2nd moment information of Eqn. 2 the original distribution of the internuclear vector cannot be reconstructed without further assumptions. One

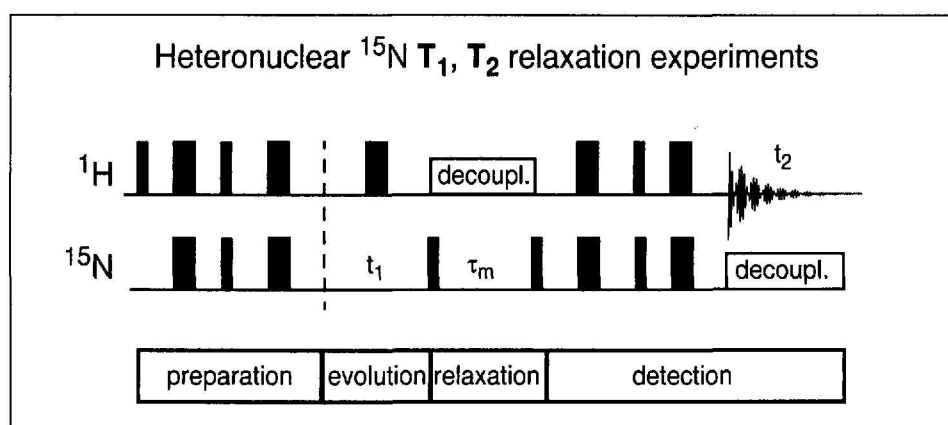


Fig. 3. Schematic representation of 2D  $^{15}\text{N}$ -NMR relaxation experiments, where the black rectangles indicate radio-frequency pulses

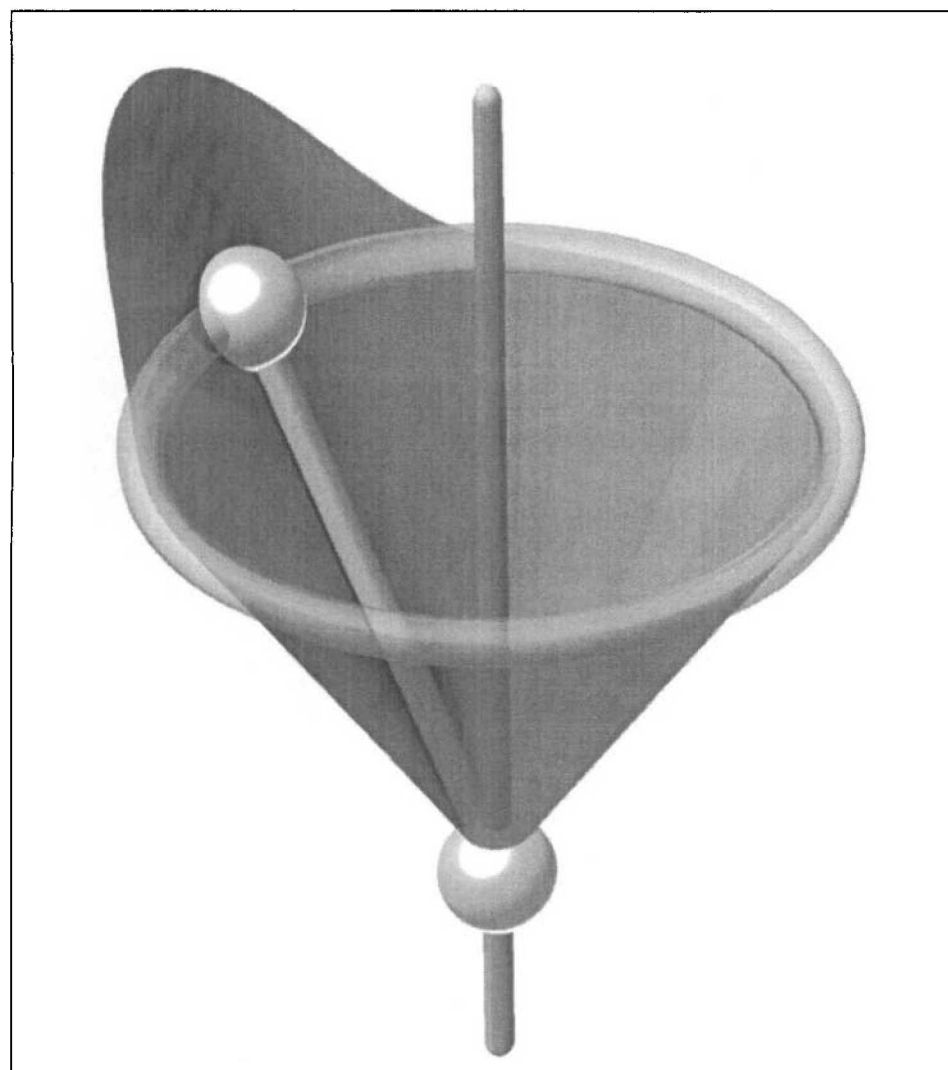


Fig. 4. Geometric view of the Gaussian Axial Fluctuation (GAF) model. The motion of the internuclear vector is modeled by Gaussian fluctuations about the vertical axis leading to the displayed distribution on the surface of a cone (reprinted with permission from [14]).



assumption, *e.g.*, that is guided by a harmonic or quasi-harmonic description of protein dynamics relevant for spin relaxation (class 3 models) [15] leads to the Gaussian axial fluctuation (GAF) model [14] belonging to the class of concrete analytical models (1), where it is assumed that the angular fluctuations of the internuclear vector is dominated by Gaussian fluctuations about a single axis (Fig. 4). For this model it is possible to analytically relate the  $S^2$ -order parameter to a dihedral angular fluctuation amplitude  $\sigma_\varphi$ :

$$S^2 = 1 - 3 \sin^2 \theta \{ \cos^2 \theta (1 - e^{-\sigma_\varphi^2}) + \frac{1}{4} \sin^2 \theta (1 - e^{-4\sigma_\varphi^2}) \} \quad (3)$$

where  $\theta$  is the constant angle between the internuclear vector and the fluctuation axis. In the limit of very large  $\sigma_\varphi$ ,  $S^2 = (3 \cos^2 \theta - 1)^2 / 4$  corresponding to unrestricted diffusion on the surface of a cone [13][16]. GAF has also been successfully applied to describe the effect of local dihedral angular fluctuations on vicinal scalar  $J$ -coupling constants [17].

Since  $S^2$  is a measure of locally sampled conformational space, it is no surprise that it also has a thermodynamic meaning. It can be shown that the differential  $S^2$  values between two different protein states A and B yields an estimate of the entropic contribution to the free energy [18]

$$\Delta G_{S^2}^{A \rightarrow B} \cong -kT \sum_J \log \frac{(1 - S_{B,J}^2)}{(1 - S_{A,J}^2)} \quad (4)$$

where the sum includes the different nuclei. This expression has been applied [18] to elucidate the contribution of changes in the fast timescale backbone dynamics of calbindin  $D_{9k}$  on calcium-binding cooperativity studied by the groups of Chazin and Forsén [19].

### An Example

A backbone  $^{15}\text{N}$ -NMR relaxation analysis was performed [20] on the protein ZF1–3, which contains the first three zinc fingers of the eukaryotic transcription factor TFIIIA [21] that binds to the control region of the 5S-RNA gene. Each of the Cys<sub>2</sub>-His<sub>2</sub>-type zinc-finger domains has 25–26 amino acids binding a zinc ion that stabilizes the well-defined tertiary structure consisting of an antiparallel  $\beta$ -sheet and a helix [22]. The zinc-finger domains are connected by two linker regions consisting of 5 amino acids each.

Analysis of the relaxation data of ZF1–3 in free solution yields for most residues

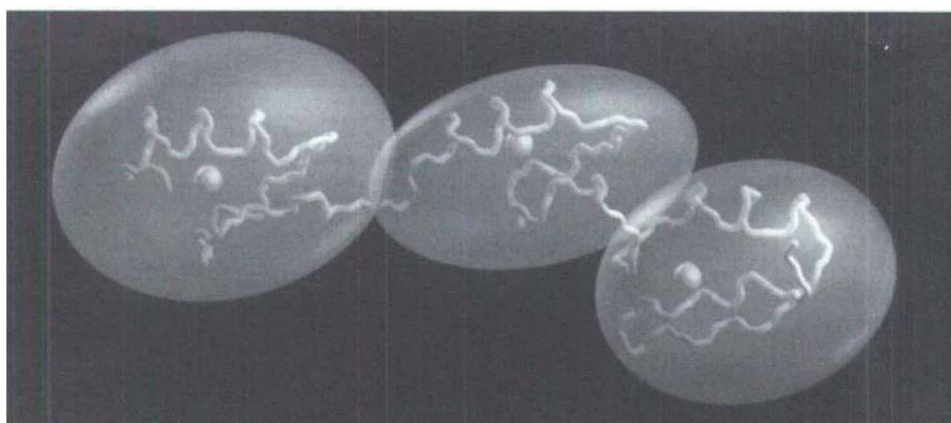


Fig. 5. Model for the average alignment of the three zinc-finger domains of ZF1–3 obtained from anisotropic rotational tumbling effects manifested in heteronuclear relaxation data. The ellipsoids superimposed on the three zinc-finger domains represent the rotational diffusion tensors for ZF1 (right), for ZF2 (middle), and for ZF3 (left) (reprinted with permission from [20]; copyright 1995, American Association for the Advancement of Science).

internal correlation times  $\tau_{int}$  below 100 ps and backbone  $S^2$ -order parameters inside the zinc-finger domains fluctuate around 0.8. According to the GAF model (Eqn. 3), this corresponds to backbone  $\varphi$ -angle fluctuation amplitudes  $\sigma_\varphi^{GAF} \leq 20^\circ$ . The two linkers exhibit somewhat increased mobility with order parameters varying between 0.6 and 0.8, *i.e.*,  $\sigma_\varphi^{GAF} \approx 20\text{--}30^\circ$ .

The explanation of overall tumbling behavior requires more sophisticated models, since the relaxation data are inconsistent with an isotropic overall tumbling behavior that is usually observed for globular proteins. Analysis of the tumbling behavior by using a quadratic form [20] of Woessner's original equations [23] shows significant anisotropic rotational diffusion for all three zinc-finger domains. In Fig. 5 the resulting rotational diffusion tensors are superimposed as ellipsoids on the backbone structure of ZF1–3. The middle finger ZF2 shows the slowest tumbling (smallest diffusion tensor) with the largest anisotropy, since it is directly restricted in its motion from both sides by ZF1 and ZF3. Thus, ZF1–3 exhibits on the 10-ns timescale a large degree of long-range motional restriction, which appears to have a direct entropic relevance for the DNA-binding process: a mutation in the linker connecting ZF1 and ZF2 leads to increased mobility of ZF1, while DNA binding is abolished. The structural information that can be derived from anisotropic tumbling may become a useful tool for structure elucidation in systems where the NOE and  $J$ -coupling density is low.

I enjoyed the collaborations with Dr. Mikael Akke, Mr. Tobias Bremi, Dr. Martin J. Blackledge, Dr. Bernhard Brutscher, Dr. David A. Case, Dr. H. Jane Dyson, Dr. Garry P. Gippert,

Prof. Christian Griesinger, Prof. Martin Karplus, Prof. Xiubei Liao, Mr. Stephan Lienin, Dr. Tom Macke, Mr. Zoltan Mádi, Dr. Gene Merutka, Dr. Dimitri Morikis, Prof. Art G. Palmer, Prof. Benoît Roux, Dr. Jürgen M. Schmidt, and Dr. Jian Yao, and I would like to thank all of them for their contributions to the work presented here and elsewhere. I am particularly indebted to Prof. Richard R. Ernst and Dr. Peter E. Wright for their advice, encouragement, and their generous support.

Received: March 6, 1997

- [1] A. Abragam, 'Principles of Nuclear Magnetism', Clarendon Press, Oxford, 1961.
- [2] 'Nuclear Magnetic Resonance Probes of Molecular Dynamics', Ed. R. Tycko, Kluwer Acad. Publ., Dordrecht, 1994.
- [3] A.G. Palmer III, J. Williams, A. McDermott, *J. Phys. Chem.* **1996**, *100*, 13293.
- [4] R.R. Ernst, G. Bodenhausen, A. Wokaun, 'Principles of Nuclear Magnetic Resonance in One and Two Dimensions', Clarendon Press, Oxford, 1987.
- [5] K. Wüthrich, 'NMR of Proteins and Nucleic Acids', John Wiley & Sons, New York, 1986.
- [6] J.N.S. Evans, 'Biomolecular NMR Spectroscopy', Oxford University Press, Oxford, 1995.
- [7] a) R.K. Wangsness, F. Bloch, *Phys. Rev.* **1953**, *89*, 728; b) A.G. Redfield, *Adv. Magn. Reson.* **1965**, *1*, 1.
- [8] R. Brüschweiler, B. Roux, M.J. Blackledge, C. Griesinger, M. Karplus, R.R. Ernst, *J. Am. Chem. Soc.* **1992**, *114*, 2289.
- [9] R. Brüschweiler, D.A. Case, *Prog. NMR Spectrosc.* **1994**, *26*, 27.
- [10] a) R. Brüschweiler, M.J. Blackledge, R.R. Ernst, *J. Biomol. NMR* **1991**, *1*, 3; b) M.J. Blackledge, R. Brüschweiler, C. Griesinger, J.M. Schmidt, P. Xu, R.R. Ernst, *Biochemistry* **1993**, *32*, 10960.
- [11] a) W. Bürgermeister, T. Wieland, R. Winkler, *Eur. J. Biochem.* **1974**, *44*, 311; b) H. Kessler, C. Griesinger, J. Lantz, A. Müller,

- W.F. van Gunsteren, H.C.J. Berendsen, *J. Am. Chem. Soc.* **1988**, *110*, 3394.
- [12] L.E. Kay, D.A. Torchia, A. Bax, *Biochemistry* **1989**, *28*, 8972.
- [13] a) G. Lipari, A. Szabo, *J. Am. Chem. Soc.* **1982**, *104*, 4546; b) *ibid.* **1982**, *104*, 4559.
- [14] R. Brüschweiler, P.E. Wright, *J. Am. Chem. Soc.* **1994**, *116*, 8426.
- [15] a) Brüschweiler, *J. Am. Chem. Soc.* **1992**, *114*, 5341; b) A.G. Palmer, D.A. Case, *ibid.* **1992**, *114*, 9059; c) R. Brüschweiler, D.A. Case, *Phys. Rev. Lett.* **1994**, *72*, 940; d) R. Brüschweiler, *J. Chem. Phys.* **1995**, *102*, 3396.
- [16] D.E. Woessner, *J. Chem. Phys.* **1962**, *36*, 1.
- [17] a) J.C. Hoch, C.M. Dobson, M. Karplus, *Biochemistry* **1985**, *24*, 3831; b) R. Brüschweiler, D.A. Case, *J. Am. Chem. Soc.* **1994**, *116*, 11199.
- [18] M. Akke, R. Brüschweiler, A.G. Palmer, *J. Am. Chem. Soc.* **1993**, *115*, 9832.
- [19] a) M. Akke, N.J. Skelton, J. Kördel, A.G. Palmer, W.J. Chazin, *Biochemistry* **1993**, *32*, 9832; b) S. Linse, C. Johansson, P. Brodin, T. Grundström, T. Drakenberg, S. Forsén, *ibid.* **1991**, *30*, 154.
- [20] R. Brüschweiler, X. Liao, P.E. Wright, *Science* **1995**, *268*, 886.
- [21] J. Miller, A.D. McLachlan, A. Kluge, *EMBO J.* **1985**, *4*, 1609.
- [22] M.S. Lee, G.P. Gippert, K.V. Soman, D.A. Case, P.E. Wright, *Science* **1989**, *245*, 635.
- [23] D.E. Woessner, *J. Chem. Phys.* **1962**, *37*, 647.

*Chimia* 51 (1997) 144–146  
© Neue Schweizerische Chemische Gesellschaft  
ISSN 0009–4293

# Invention and Development of a Novel Catalytic Process for the Production of a Benzenesulfonic Acid-Building Block

Peter Baumeister<sup>a)</sup>\*, Willy Meyer<sup>b)</sup>, Konrad Oertle<sup>b)</sup>, Gottfried Seifert<sup>b)</sup>, and Heinz Steiner<sup>a)</sup>

(Sandmeyer Prize 1996 of the NSCS)

**Abstract.** Development of a highly 'atom-efficient' production process for 2-alkyl-substituted benzenesulfonic acids by arylation of olefins with 2-diaziobenzene sulfonate catalyzed by a homogeneous Pd-complex and subsequent hydrogenation of the resulting styrenes with an *in situ* generated heterogeneous Pd-catalyst.

the, at that time novel, Heck arylation reaction [1]. The study revealed the nowadays widely recognized applicability of the above-mentioned reaction. Since aryl bromides or iodides are in many cases not readily available as starting materials, the research group started to explore other leaving groups [2] in order to generate the Pd-aryl species prerequisite to the insertion of the olefin ligands.

Konrad Oertle, at that time member of the 'Catalysis Research' group explored the so-called Matsuda [3] reaction (Scheme 1). This reaction type starts from the diazonium salts of aromatic amines as a precursor for the Pd-aryl species. He realized the very broad scope of this reaction and, after optimization of the reaction conditions, synthesized a broad variety of substituted styrenes. This is exemplified by a series of *ortho*-substituted benzenesulfonic acids (Table) obtained from substituted olefins by arylation with 2-diaziobenzene sulfonate.

## 1. Introduction

Industrial R&D in contrast to research in academia is directed to generate added value for the company and their customers, either by discovery of products with outstanding properties or by finding new and more economic ways to produce these goods. The story to tell is about how catalysis as a *Technology* can facilitate both, the discovery of a new product and the development of a new and economic process.

## 2. Discovery of an Useful Intermediate

In the early eighties in the catalysis group of Ciba-Geigy's Central Research Laboratories, a program was induced in order to exploit the synthetic potential of

## 3. Invention of a New Herbicide

At the same time, Willy Meyer, a chemist in R&D of Ciba's 'Crop Protection Division', worked on a project in the field of sulfonylurea herbicides, a field well



v.l.n.r. P. Baumeister, H. Steiner, K. Oertle, W. Meyer, G. Seifert

Foto: R. Hauck, Basel

\*Correspondence: P. Baumeister  
Novartis Services AG  
R-1055.6.62  
CH-4002 Basel

<sup>a)</sup> Scientific Services, Novartis Services AG  
CH-4002 Basel

<sup>b)</sup> Novartis Crop Protection AG  
CH-4002 Basel